Pion and kaon valence-quark parton distribution functions

Trang Nguyen,[1] Adnan Bashir,[2,3] Craig D. Roberts,[3,4,5] and Peter C. Tandy[3]

[1]*Center for Nuclear Research, Department of Physics, Kent State University, Kent, Ohio 44242, USA*

[2]*Instituto de Física y Matemáticas, Universidad Michoacana de San Nicolás de Hidalgo, Morelia, Michoacán 58040, Mexico*

[3]*Kavli Institute for Theoretical Physics China, CAS, Beijing 100190, China*

[4]*Physics Division, Argonne National Laboratory, Argonne, Illinois 60439, USA*

[5]*Department of Physics, Center for High Energy Physics and the State Key Laboratory of Nuclear Physics and Technology,*

Peking University, Beijing 100871, China

A rainbow-ladder truncation of QCD's Dyson-Schwinger equations, constrained by existing applications to hadron physics, is employed to compute the valence-quark parton distribution functions of the pion and kaon. Comparison is made to π-N Drell-Yan data for the pion's u-quark distribution and to Drell-Yan data for the ratio $u_K(x)/u_\pi(x)$: the environmental influence of this quantity is a parameter-free prediction, which agrees well with existing data. Our analysis unifies the computation of distribution functions with that of numerous other properties of pseudoscalar mesons.

Experimental information on the quark and gluon parton distribution functions (PDF) in the pion have primarily been inferred from the Drell-Yan reaction [1–3] in pion-nucleon and pion-nucleus collisions. Kaon PDF data exist in the form of the ratio $u_K(x)/u_\pi(x)$ [1,4]. While the nucleon PDFs are now fairly well determined, the pion and kaon PDFs remain poorly known. Reference [5] reviews both the experimental and theoretical status of nucleon and pion PDFs. Since the pion is central to hadron physics, and its key characteristics are dictated by dynamical chiral symmetry breaking, pion structure is a critical testing ground for our understanding of nonperturbative QCD. Much more theoretical work has been devoted to the pion elastic charge form factor (e.g., [6]), $\pi\pi$ scattering (e.g., [7]), and the pion electromagnetic transition form factor (e.g., [8]) than has been devoted to the pion PDFs. Herein we take a material step toward ameliorating that deficit.

Lattice-regularized QCD is restricted to low-order moments of the PDFs: the pointwise x dependence is not directly accessible [5,9], and model calculations of PDFs are challenging. Chiral symmetry has guided studies of pion PDFs within the Nambu–Jona-Lasinio (NJL) model [10] at the expense of an unphysical point-particle structure for the pion Bethe-Salpeter amplitude, and ambiguities from a dependence upon regularization procedure owing to the lack of renormalizability. Constituent quark models [11], instanton-liquid models [12], and semiempirical hadronic Fock state expansion models [13] have also been used, with the last reporting results for $u_K(x)/u_\pi(x)$, too. In all these approaches, it is difficult to have pQCD elements coexisting naturally with nonperturbative aspects of a bound state while respecting the quantum field theoretical nature of the underlying dynamics. The large x behavior of the pion PDFs provides an illustration. The QCD parton model [14] and pQCD [15] are clear: at a scale of order-$\Lambda_{\rm QCD}$ the behavior is $u_\pi(x) \propto (1-x)^\alpha$ with $\alpha = 2 + \gamma$ where $\gamma > 0$ is a logarithmic correction. However the above models imply an α ranging from 0 to 1, or at most 1.5 [5].

These issues may in principle be addressed if the PDFs can be obtained from truncations of QCD's Dyson-Schwinger equations (DSEs). The DSEs are a hierarchy of coupled integral equations for the Schwinger functions (n-point functions) of a theory. Bound states appear as poles in the appropriate n-point functions; e.g., the bound-state Bethe-Salpeter equation (BSE) of field theory appears after taking residues in the inhomogeneous DSE for the appropriate color singlet vertex. Numerous reviews, e.g., [16], describe the insight into hadron physics achieved through the use of the rainbow-ladder (RL) truncation of the DSEs, which is the leading order in a systematic, symmetry-preserving scheme [17].

The first DSE study of PDFs was conducted for the pion [18] in an analysis that employed phenomenological parametrizations of both the Bethe-Salpeter amplitude and dressed-quark propagators. The purpose of this present work is to employ numerical DSE solutions in the computation of the pion and kaon PDFs, utilizing the same RL model that successfully predicted electromagnetic form factors [6,19–21]; and to study the ratio $u_K(x)/u_\pi(x)$ in order to elucidate aspects of the influence of a hadronic environment.

In the Bjorken limit, deep inelastic scattering selects the most singular behavior of a correlator of quark fields of the target with light-like and causal distance separation $z^2 \sim 0^+$. With incident photon momentum along the negative three-axis, the kinematics selects $z^+ \sim z_\perp \sim 0$, leaving z^- as the finite distance conjugate to the quark momentum component xP^+, where $x = Q^2/2P \cdot q$ is the Bjorken variable, $q^2 = -Q^2$ is the spacelike virtuality of the photon, and P is the target momentum. To leading order in the operator product expansion, the target structure functions are proportional to the charge-weighted sum of PDFs, $q_f(x)$, for parton of flavor f. The PDF is given by the correlator [22,23]

$$q_f(x) = \frac{1}{4\pi} \int d\lambda\, e^{-ixP\cdot n\lambda} \langle \pi(P)| \bar{\psi}_f(\lambda n)\, \slashed{n}\, \psi_f(0)|\pi(P)\rangle_c,$$

<div align="right">(1)</div>

expressed here in manifestly Lorentz-invariant form. In the infinite momentum frame, $q_f(x)$ is the probability that a single f-parton has momentum fraction $x = k \cdot n/P \cdot n$ [23]. In the above, n^μ and (for later use) p^μ are light-like vectors satisfying $n^2 = p^2 = 0$ and $n \cdot p = 2$. They form a convenient basis for the longitudinal sector of four-vectors. One has $k \cdot n = k^+$ and $k \cdot p = k^-$. The dominant component of q is parallel to n, i.e., q^- dominates. Note that $q_f(x) = -q_{\bar{f}}(-x)$, and that the valence quark amplitude is $q_f^v(x) = q_f(x) - q_{\bar{f}}(x)$. It follows from Eq. (1) that $\int_0^1 dx\, q_f^v(x) = \langle \pi(P)|J_f^+(0)|\pi(P)\rangle/2P^+ = F_\pi(0) = 1$.

In our DSE framework, dynamical information on the various nonperturbative elements, such as propagators and bound-state amplitudes, is available in a Euclidean momentum representation. (In our Euclidean metric: $\{\gamma_\mu, \gamma_\nu\} = 2\delta_{\mu\nu}$, $\gamma_\mu^\dagger = \gamma_\mu$, $\gamma_5 = \gamma_4\gamma_1\gamma_2\gamma_3$, $a \cdot b = \Sigma_{i=1}^4 a_i b_i$, $\not{n} = \gamma \cdot n$, and P_μ timelike $\Rightarrow P^2 < 0$.) The corresponding formulation of Eq. (1) is

$$q_f(x) = -\frac{1}{2}\int \frac{d^4k}{(2\pi)^4}\delta(k \cdot n - xP \cdot n)\,\mathrm{tr}_{cd}[i\not{n}\, G(k, P)], \quad (2)$$

where tr_{cd} denotes a color and Dirac trace, and $G(k, P)$ represents the forward $\bar{q}$-target scattering amplitude. In Euclidean metric the vectors n, p, P satisfy $n^2 = 0 = p^2$, $n \cdot p = -2$, $P^2 = -m_\pi^2$, and $P \cdot n = -m_\pi$.

The top part of Fig. 1 illustrates Eq. (2). In rainbow-ladder truncation, which sums a symmetry-preserving subset of dressed-quark and -gluon contributions to the bound state, we have the decomposition illustrated in the bottom part of Fig. 1. The four-point function S_2 is the dressed-$q\bar{q}$ two-body propagator and Γ_π is the Bethe-Salpeter bound-state amplitude, both computed in the RL truncation. The schematic form $\int d^4k\, S_2 \otimes i\not{n}\,\delta(k \cdot n - xP \cdot n) = S(\ell)\,\Gamma^n(\ell; x)\,S(\ell)$ is one way to specify the required dressed-quark vector vertex $\Gamma^n(\ell; x)$. The RL truncation of Eq. (2) for the valence $u_\pi(x)$ is thus

$$u_\pi(x) = -\frac{1}{2}\int \frac{d^4\ell}{(2\pi)^4}\mathrm{tr}_{cd}\,[\Gamma_\pi(\ell, -P) \\ \times S_u(\ell)\,\Gamma^n(\ell; x)\,S_u(\ell)\,\Gamma_\pi(\ell, P)\,S_d(\ell - P)]\,, \quad (3)$$

where the dressed-quark propagator is $S(\ell; \zeta) = 1/[i\not{\ell}\, A(\ell^2; \zeta) + B(\ell^2; \zeta)]$, with ζ being the renormalization mass scale. Note that the $\int d^4k$ evident in Fig. 1 is contained
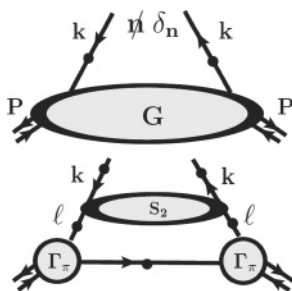

FIG. 1. Diagrammatic representation of parton distributions. Top panel: the exact parton distribution corresponding to Eq. (2). Bottom panel: Rainbow-ladder truncation of the amplitude G. S_2 is the $q\bar{q}$ propagator.

within the definition of $\Gamma^n(\ell; x)$. This vertex satisfies an inhomogeneous BSE (here with a RL kernel) specified by the driving term $i\not{n}\,\delta(\ell \cdot n - xP \cdot n)$.

This selection of dynamics is an exact parallel to the RL treatment of the pion charge form factor at $Q^2 = 0$, wherein the dressed vertex is defined with the inhomogeneous term $i\gamma_\mu$. Chiral symmetry and vector current conservation are preserved [6,19]. Equation (3) ensures $\int_0^1 dx\, q_f^v(x) = 1$ for $f = u, \bar{d}$ automatically since $\int dx\,\Gamma^n(\ell; x)$ gives the Ward identity vertex and the result follows from canonical normalization of the BS amplitude.

We adopt the representation $\ell^\mu = \frac{1}{2}(\alpha p^\mu + \beta n^\mu) + k_\perp^\mu$ to transform to new variables $\alpha = -\ell \cdot n$ and $\beta = -\ell \cdot p$, thus converting Eq. (3) to the form

$$u_\pi(x) = \frac{-J_E}{2(2\pi)^4}\int_{-\infty}^{+\infty} d\beta\, d^2\ell_\perp\, T(n, p; \ell, P)|_{\alpha=xP \cdot n}, \quad (4)$$

where $J_E = -i/2$ is the Jacobian of the variable transformation; and T is the result of the trace in Eq. (3), using $\Gamma^n(\ell; x) \approx n_\mu \partial S^{-1}(\ell)/\partial \ell_\mu\,\delta(\ell \cdot n - xP \cdot n)$, which is the correct result from the Ward identity after $\int dx$.

Since $q_f(x)$ is obtained from the hadron tensor $W^{\mu\nu}$, which in turn can be formulated from the discontinuity $T^{\mu\nu}(\epsilon) - T^{\mu\nu}(-\epsilon)$ of the forward Compton amplitude $T^{\mu\nu}$, we observe that all enclosed singularities from the difference of contours cancel except for the cut that produced the δ-function constraint on α.

We employ the RL-DSE model developed in Refs. [24–26], in which the BSE kernel takes the form $K = -4\pi\,\alpha_{\mathrm{eff}}(k^2)\, D_{\mu\nu}^{\mathrm{free}}(k)\frac{\lambda^i}{2}\gamma_\mu \otimes \frac{\lambda^i}{2}\gamma_\nu$, where k is the gluon momentum. The parameters used here are exactly as listed in Ref. [26]; besides the current quark masses, there is one infrared strength parameter for $\alpha_{\mathrm{eff}}(k^2)$ and it reproduces QCD's one-loop renormalization-group behavior for $k^2 \gtrsim 2\,\mathrm{GeV}^2$. A more general method for treating K has recently become available [27]. The DSE that produces $S(\ell)$ is also determined by $\alpha_{\mathrm{eff}}(k^2)$ [24–26]; and the combination of the DSE and BSE produces dressed color-singlet vector and axial-vector vertices satisfying their respective Ward-Takahashi identities. This ensures that the chiral limit ground-state pseudoscalar bound states are the massless Goldstone bosons from dynamical chiral symmetry breaking [24,25]; and it ensures electromagnetic current conservation [28]. This kernel is found to be successful for, among other things, light-quark meson properties [26], including electromagnetic elastic [6,19] and transition [20,21] form factors. Selected pion and kaon results are displayed in Table I.

For $\Gamma_\pi(\ell, P)$ we employ the most general form,

$$i\Gamma_\pi(\ell, P) = \gamma_5\,[i E_\pi(q; P) + \not{P} F_\pi(q; P) \\ + \not{q}\, G_\pi(q; P) + \sigma_{\mu\nu}q_\mu P_\nu H_\pi(q; P)]\,, \quad (5)$$

where $q = \ell - P/2$ is the relative $q\bar{q}$ momentum appropriate to Eq. (3). For a charge-conjugation eigenstate (e.g., the pion), the invariant amplitudes E, F, and H are even in $q \cdot P$, while G is odd. The kaon invariant amplitudes contain both even and odd components. We expand the $q \cdot P$ dependence in Chebyshev polynomials [26], keeping terms of order

TABLE I. Illustrative selection of DSE results [6,19,20,26] obtained with the RL kernel employed herein compared with experimental values [29]. (Dimensioned quantities are listed in GeV or fm^2, as appropriate.)

	m_π	f_π	m_K	f_K	r_π^2	$r_{K^+}^2$	$g_{\pi\gamma\gamma}$	$r_{\pi\gamma\gamma}^2$
Expt.	0.138	0.092	0.496	0.113	0.44	0.34	0.5	0.42
Calc.	0.138	0.092	0.497	0.110	0.45	0.38	0.5	0.41

$n = 0 - 3$. The domain of ℓ^2 over which the quark propagators are needed in this application is larger than what is available from previous solutions of the quark DSE. We therefore adopt a constituent mass pole approximation for the denominator of the spectator quark propagator [18]. Constituent spectator masses $(M_u, M_s) = (0.4, 0.55)$ GeV permit a minimal adjustment to establish the normalization $\langle x^0 \rangle$. We compared the approximation $\Gamma^n(\ell; x) \approx n_\mu \partial S^{-1}(\ell)/\partial \ell_\mu \, \delta(\ell \cdot n - x P \cdot n)$ with the bare vertex truncation and found that no distribution moment changed by more than 3%. This approximation becomes exact in the limit of an infrared dominant RL kernel [30].

In Fig. 2 we display our DSE result [31] for the valence u-quark distribution evolved to $Q^2 = (5.2 \, \text{GeV})^2$ in comparison with πN Drell-Yan data [3] at a scale $Q^2 \sim (4.05 \, \text{GeV})^2$ obtained via a LO analysis. Our distribution at the model scale Q_0 is evolved using leading-order DGLAP. The model scale is fixed to $Q_0 = 0.57$ GeV by matching the x^n moments for $n = 1, 2, 3$ to the experimental analysis given at $(2 \, \text{GeV})^2$ [34]. Our momentum sum rule result $\langle x \rangle_{u+d} = 0.74$ (pion), $\langle x \rangle_{u+s} = 0.76$ (kaon) at Q_0 shows clearly the implicit inclusion of gluons as a dynamical entity in a true covariant bound-state approach.
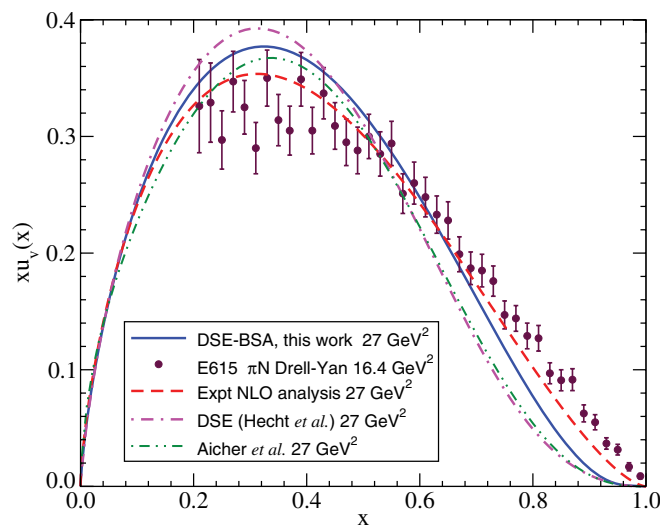
Only a point-meson BS amplitude can produce a value of 1.0 for the momentum sum rule at Q_0 [8].

In Fig. 2 we also show the result from the first DSE study [18], which employed phenomenological parametrizations of the nonperturbative elements. Our present calculation lies marginally closer to the Drell-Yan data in Ref. [3] at high x. However, this is not significant because both DSE results agree with pQCD; viz., $u(x) \sim (1 - x)^\alpha$ with $\alpha \gtrsim 2$ and growing with increasing scale, which is not true of the reported Drell-Yan data.

Motivated by this, a NLO reanalysis of the data was performed [32]; and we also show that result at $Q^2 = (5.2 \, \text{GeV})^2$ in Fig. 2. It does clearly reduce the extracted PDF at high x but not enough to resolve the data's apparent discrepancy with pQCD behavior, which is discussed at length in Ref. [5]. The DSE exponents are 2.4 at model scale $Q_0 = 0.54$ GeV in Ref. [18], and 2.1 at scale $Q_0 = 0.57$ GeV for the present study. DSE analyses do not allow much room for a larger PDF at high x. A resolution of the conflict between data and well-constrained theory has recently been proposed: a reanalysis of the original data at NLO with a resummation of soft gluon processes [33] produces a PDF whose behavior for $x > 0.4$ is essentially identical to that of the earlier DSE calculation [18], as is apparent in Fig. 2.

In Fig. 3 we display the first nine moments of our result for $u_\pi(x)$ at scale $Q^2 = (5.2 \, \text{GeV})^2$ in comparison with the earlier DSE result from Ref. [18] and the NLO reanalysis [32] of the original E615 data, all plotted as a percent deviation from the moments of the most recent analysis in Ref. [33]. Considering that the high moments are small, e.g., $\langle x^9 \rangle \sim 0.003$, the two DSE results are both equally well in accord with the recent analysis.

The ratio u_K/u_π measures the local hadronic environment. In the kaon, the u quark has a heavier partner than in the pion, and this should cause $u(x)$ to peak at lower x in the kaon. Our

FIG. 2. (Color online) Pion valence quark distribution function evolved to $(5.2 \, \text{GeV})^2$. Solid curve: full DSE calculation [31]; dot-dashed curve: semi-phenomenological DSE-based calculation in Ref. [18]; filled circles: experimental data from Ref. [3], at scale $(4.05 \, \text{GeV})^2$; dashed curve: NLO reanalysis of the experimental data [32]; and dot-dot-dashed curve: NLO reanalysis of experimental data with inclusion of soft-gluon resummation [33].
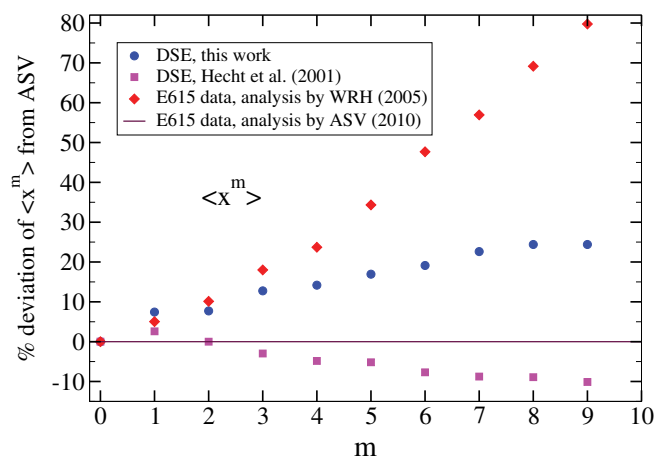

FIG. 3. (Color online) Moments of the pion's valence $u(x)$ at scale $(5.2 \, \text{GeV})^2$, shown as a percent deviation from the recent (ASV) reanalysis [33] (NLO, with soft gluon resummation) of the 1989 E615 πN Drell-Yan data [3]. Filled circles: present full DSE calculation [31]; filled squares: semi-phenomenological DSE-based calculation [18]; and filled diamonds: reanalysis (NLO, without soft gluon resummation) of the same Drell-Yan data [32].
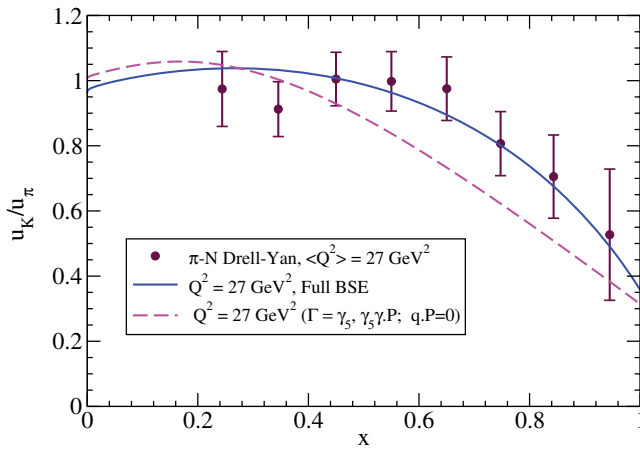
FIG. 4. (Color online) DSE prediction for the ratio of u-quark distributions in the kaon and pion [5,31]. The full Bethe-Salpeter amplitude produces the *solid* curve; the reduced BS amplitude produces the *dashed* curve. The reduced amplitude retains only the invariants and amplitudes involving pseudoscalar and axial vector Dirac matrices, and ignores dependence on the variable $q \cdot P$. These are part of the reductions that occur in a pointlike treatment of the pseudoscalar mesons. The experimental data are from [1,4].

DSE calculation [31] is shown in Fig. 4 along with available Drell-Yan data [1,4], which does not separate sea and valence quarks. Our parameter-free result agrees well with the data. The ratio at $x = 0$ approaches one under evolution owing to the increasingly large population of sea quarks produced thereby [35]. On the other hand, the ratio at $x = 1$ is a fixed point under evolution; i.e., it is independent of the scale Q^2, and is therefore a persistent probe of nonperturbative dynamics [5].

In Fig. 4 we also display a calculation which employs a reduced BS amplitude: only the leading two invariant amplitudes $E(q; P)$ and $F(q; P)$ are retained, and each is truncated to the lowest Chebyshev moment in $q \cdot P$, i.e., $E(q; P) \to \tilde{E}(q^2)$. The field theory variable $q \cdot P$ is a constant in quantum mechanics. (These reductions in the BSE vertices occur within a NJL model description; but that model also ignores the q^2 dependence of the vertices.) These simplifications do not change the qualitative behavior of the ratio, but the detailed quantitative agreement is impaired.

An estimate of the leading large-x behavior $u_K(x) \sim A_K (1-x)^\alpha$ can be made in the limit where the quark propagators are characterized by constituent masses M_u, M_s and the vertex is taken to be $i \not{n} \, \delta(\ell \cdot n - x P \cdot n)$, preserving the Ward identities. We also truncate Γ_K to $\gamma_5 E_K(q^2) = \gamma_5 N_K/(q^2 + \Lambda_K^2)$ where $q = \ell - P/2$. The quark mass dependence of A_K and A_π will provide an estimate of $u_K(1)/u_\pi(1)$. For $x > 1/2$ the pole in the spectator quark propagator is the only one in the upper half plane and the ℓ^- integral may readily be evaluated to yield

$$u_K(x) = \frac{4 N_c \pi^2}{(2\pi)^4} \int_{\mu_m(x)}^{\infty} d\mu \, \frac{x \, \mathcal{M}^2 + \mu + M_u^2}{\left[\mu + M_u^2 \right]^2} \, E_K^2(q^2). \quad (6)$$

Here $\mathcal{M}^2 = m_K^2 - (M_s - M_u)^2$; we have changed the integration variable from $\vec{\ell}_\perp$ to $\mu = -\ell^2$, where the latter is the value at the ℓ^- pole; q^2 evaluated at the ℓ^- pole is $q^2 = m_K^2/4 + (\mu - M_s^2)/2$; and $\mu_m(x) = a/(1-x) - x m_K^2$, with $a = x M_s^2$. This divergence of the lower limit for large x guarantees that the result is completely determined by the ultraviolet behavior of the propagators and bound-state amplitudes.

The integral can be expressed as

$$u_K(x) = N \int_0^{\infty} d\hat{\mu} \, \frac{\frac{a}{1-x} + b + \hat{\mu}}{\left[\frac{a}{1-x} + c + \hat{\mu} \right]^2} \left(\frac{a}{1-x} + d + \hat{\mu} \right)^{-n}, \quad (7)$$

where bound-state amplitudes determined by one gluon exchange correspond to $n = 2$. The quantities a, b, c, d depend on the mass-dimensioned scales in the system and are nonsingular in x: a scales with the square of the spectator quark mass and other details are immaterial. A change of variable to $\bar{\mu} = (1-x)\hat{\mu}/a$ shows that $u_K(x) \propto [(1-x)/a]^n$ when $a/(1-x)$ is greater than any physical mass scale in the system. Running of the struck quark mass over a wide domain can be accommodated. We thus have $u_K(x) \propto N_K^2 (1-x)^2/M_s^4$ and $u_\pi(x) \propto N_\pi^2 (1-x)^2/M_u^4$. Note that it is the bound-state amplitudes that completely determine the exponent α [5]: if the argument of $E_{K/\pi}$ did not diverge at large x, the combined scaling effect of the propagators would vanish, giving $\alpha = 0$.

The above analysis applied to the ratio suggests $u_K(1)/u_\pi(1) \sim \frac{f_\pi^2}{f_K^2} (M_u/M_s)^4 \sim 0.3$, where the ratio of Bethe-Salpeter amplitude normalization constants is estimated from our computed f_π/f_K. This estimate is in fair accord with our full calculation in Fig. 4. The NJL model with a sharp cutoff yields $(M_u/M_s)^2$ [10]. However, in general this lacks a physical contribution from bound-state amplitudes and NJL results depend sensitively upon the regularization scheme.

With this study we have unified the computation of distribution functions that arise in analyses of deep inelastic scattering with that of numerous other properties of pseudoscalar mesons, including meson-meson scattering and the successful prediction of electromagnetic elastic and transition form factors. Our results confirm the large-x behavior of distribution functions predicted by the QCD parton model and provide a good account of the π-N Drell-Yan data for $u_\pi(x)$; and our parameter-free prediction for the ratio $u_K(x)/u_\pi(x)$ agrees with extant data, showing a strong environment dependence of the u-quark distribution.

[1] J. Badier *et al.* (NA3 Collaboration), Z. Phys. C **18**, 281 (1983).
[2] B. Betev *et al.* (NA10 Collaboration), Z. Phys. C **28**, 15 (1985).
[3] J. S. Conway *et al.*, Phys. Rev. D **39**, 92 (1989).
[4] J. Badier *et al.* (Saclay-CERN-College de France-Ecole Poly-Orsay Collaboration), Phys. Lett. B **93**, 354 (1980).
[5] R. J. Holt and C. D. Roberts, Rev. Mod. Phys. **82**, 2991 (2010).
[6] P. Maris and P. C. Tandy, Phys. Rev. C **62**, 055204 (2000).
[7] P. Bicudo *et al.*, Phys. Rev. D **65**, 076008 (2002).
[8] H. L. L. Roberts, C. D. Roberts, A. Bashir, L. X. Gutierrez-Guerrero, and P. C. Tandy, Phys. Rev. C **82**, 065202 (2010).
[9] C. Best *et al.*, Phys. Rev. D **56**, 2743 (1997); W. Detmold, W. Melnitchouk, and A. W. Thomas, *ibid.* **68**, 034025 (2003).
[10] T. Shigetani, K. Suzuki, and H. Toki, Phys. Lett. B **308**, 383 (1993); H. Weigel, E. Ruiz Arriola, and L. P. Gamberg, Nucl. Phys. B **560**, 383 (1999); W. Bentz, T. Hama, T. Matsuki, and K. Yazaki, Nucl. Phys. A **651**, 143 (1999); R. M. Davidson and E. Ruiz Arriola, Acta Phys. Pol. B **33**, 1791 (2002).
[11] A. Szczepaniak, C. R. Ji, and S. R. Cotanch, Phys. Rev. D **49**, 3466 (1994); T. Frederico and G. A. Miller, *ibid.* **50**, 210 (1994).
[12] A. E. Dorokhov and L. Tomio, Phys. Rev. D **62**, 014016 (2000).
[13] C. Avila, J. C. Sanabria, and J. Magnin, Phys. Rev. D **66**, 034016 (2002).
[14] G. R. Farrar and D. R. Jackson, Phys. Rev. Lett. **35**, 1416 (1975).
[15] S. J. Brodsky, M. Burkardt, and I. Schmidt, Nucl. Phys. B **441**, 197 (1995); X. Ji, J. P. Ma, and F. Yuan, Phys. Lett. B **610**, 247 (2005).
[16] C. D. Roberts and A. G. Williams, Prog. Part. Nucl. Phys. **33**, 477 (1994); P. C. Tandy, *ibid.* **39**, 117 (1997); C. D. Roberts and S. M. Schmidt, *ibid.* **45**, S1 (2000); P. Maris and C. D. Roberts, Int. J. Mod. Phys. E **12**, 297 (2003); L. Chang and C. D. Roberts, arXiv:1003.5006 [nucl-th].
[17] H. J. Munczek, Phys. Rev. D **52**, 4736 (1995); A. Bender, C. D. Roberts, and L. von Smekal, Phys. Lett. B **380**, 7 (1996).
[18] M. B. Hecht, C. D. Roberts, and S. M. Schmidt, Phys. Rev. C **63**, 025213 (2001).
[19] P. Maris and P. C. Tandy, Phys. Rev. C **61**, 045202 (2000).
[20] P. Maris and P. C. Tandy, Phys. Rev. C **65**, 045211 (2002).
[21] A. Höll, A. Krassnigg, P. Maris, C. D. Roberts, and S. V. Wright, Phys. Rev. C **71**, 065204 (2005).
[22] R. L. Jaffe, Nucl. Phys. B **229**, 205 (1983); in *Proceedings of the Los Alamos School on Quark Nuclear Physics*, Los Alamos, NM, Jun 10–14, 1985, edited by M. B. Johnson and A. Picklesimer (Wiley, New York, 1986).
[23] R. K. Ellis, W. J. Stirling, and B. R. Webber, *QCD and Collider Physics*, Cambridge Monographs on Particle Physics, Nuclear Physics and Cosmology Vol. 8 (Cambridge University Press, Cambridge, England, 1996), p. 1.
[24] P. Maris, C. D. Roberts, and P. C. Tandy, Phys. Lett. B **420**, 267 (1998).
[25] P. Maris and C. D. Roberts, Phys. Rev. C **56**, 3369 (1997).
[26] P. Maris and P. C. Tandy, Phys. Rev. C **60**, 055214 (1999).
[27] L. Chang and C. D. Roberts, Phys. Rev. Lett. **103**, 081601 (2009).
[28] C. D. Roberts, Nucl. Phys. A **605**, 475 (1996).
[29] K. Nakamura *et al.* (Particle Data Group), J. Phys. G **37**, 075021 (2010).
[30] H. J. Munczek and A. M. Nemirovsky, Phys. Rev. D **28**, 181 (1983).
[31] T. T. Nguyen, Ph.D. dissertation, Kent State University, 2010.
[32] K. Wijesooriya, P. E. Reimer, and R. J. Holt, Phys. Rev. C **72**, 065203 (2005).
[33] M. Aicher, A. Schafer, and W. Vogelsang, Phys. Rev. Lett. **105**, 252003 (2010).
[34] P. J. Sutton, A. D. Martin, R. G. Roberts, and W. J. Stirling, Phys. Rev. D **45**, 2349 (1992).
[35] L. Chang and C. D. Roberts, AIP Conf. Proc. **1261**, 25 (2010).